Chemical Papers (2024) 78:1415–1434
https://doi.org/10.1007/s11696-023-03168-6

ORIGINAL PAPER

# A realistic approach to radiation-induced treatment of micropollutants in wastewater

Ayşenur Genç[1] · Ece Ergun[2] · Ömer Kantoğlu[2] · Mahir İnce[3] · Orhan Acar[1]

Received: 19 June 2023 / Accepted: 22 October 2023 / Published online: 7 November 2023


## Abstract

In this study, radiation-induced removal of micropollutants commonly found in real wastewater effluents was investigated. The study began by thoroughly developing a validated analytical methodology for the determination of 13 selected micropollutants in real wastewater effluent. It was found that the concentrations of 10 target micropollutants in effluent samples were found to be above the method detection limits. The samples were then exposed to gamma radiation at several doses ranging from 0 to 50 kGy. After 30 kGy irradiation, a decrease of 100%, 5%, and 43% was observed in color, pH, and TOC, respectively. When a dose of 10 kGy was applied, estrone, 17-$\beta$-estradiol, and 4-octylphenol were not detected in irradiated wastewater samples. The removal efficiencies of other target micropollutants drastically increased with the increased dose up to 10 kGy for ibuprofen (86%), 20 kGy for diclofenac (93%), diphenylamine (79%), triclosan (98%), and bisphenol-A (97%), and 30 kGy for ketoprofen (78%) and diethyl phthalate (83%). The lowest absorbed dose required for 90% removal was found for triclosan (10.49 kGy). G-values, dose rates, and $D_{0.5}$ and $D_{0.9}$ doses depended on the initial concentration and molecular structure of the target micropollutants. In comparison with the literature data, the relatively high doses required to achieve high removal efficiencies indicate the competitive reactions for reactive species between the trace-level quantities of micropollutants and the matrix components in real wastewater. In light of this, it is suggested that research employing real wastewater samples rather than synthetic water provides more realistic results for radiation treatment applications.

**Keywords** Micropollutants · Wastewater · Ionizing radiation · G-value · Liquid chromatography · Mass spectrometry

## Introduction

Micropollutants (MPs) that appear at trace levels in the aquatic environment have become a matter of great concern due to their widespread distribution. These compounds are continuously released into the environment, whether intentionally or unintentionally, owing to weak regulatory standards, especially in developing countries (Besha et al. 2017; Chavoshani et al. 2020). Thus, MPs are found in the μg $L^{-1}$ or ng $L^{-1}$ concentration range in the aquatic environment and are considered potential threats to environmental ecosystems, including short-term and long-term toxicity (Bhatt et al. 2022; Shao et al. 2019) endocrine-disrupting effects (Varjani and Sudha 2020; Kuckelkorn et al. 2018) and antibiotic resistance of microorganisms (Bírošová et al. 2020; Välitalo et al. 2017; Stasinakis and Gatidou 2010).

The MPs are also a major issue for conventional wastewater treatment plants. Despite the numerous treatment technologies used in wastewater treatment facilities, they cannot be totally eliminated. For example, it was reported that ketoprofen and diclofenac, the most widely used pharmaceuticals, were not decomposed completely by the activated sludge system for 8 h, which is the average reaction time of the aeration tank in a real wastewater treatment plant (Kimura et al. 2012). As a result, wastewater effluents continue to pose major hazards to groundwater and surface water (Khan et al. 2022; de Santiago-Martín et al. 2020; Aydin et al. 2019). To reduce the health concerns posed by contaminants in wastewater, advanced and novel

✉ Ece Ergun
ergunlady@gmail.com

[1] Department of Chemistry, Graduate School of Natural and Applied Science, Gazi University, 06500 Ankara, Turkey

[2] Nuclear Energy Research Institute, Turkish Energy, Nuclear and Mineral Research Agency, 06983 Kahramankazan, Ankara, Turkey

[3] Department of Environmental Engineering, Gebze Technical University, 41400 Kocaeli, Turkey

technologies need to be adopted (Kumar et al. 2022; Ahmed et al. 2021; Rizzo et al. 2019).

Advanced oxidation processes (AOPs) have received increasing attention in both the science and practice of water and wastewater treatment over the past few decades due to their potential to convert organic pollutants into biodegradable compounds as well as disinfection, decolorization, and deodorization (Sievers 2011). AOPs, which appeared in addition to routine purification processes such as biological treatment, coagulation, sedimentation, and filtration, have been based on the oxidation of organic impurities by hydroxyl radicals formed from the reaction of an oxidant (Gwenzi et al. 2022). One of the most promising AOPs for removing pollutants from wastewater is radiation technology (Wang et al. 2019). When dilute aqueous solutions (at millimolar or lower concentrations of dissolved solutes) are irradiated with gamma-rays, practically large fraction of the absorbed radiation energy is deposited in water molecules. This interaction leads to the formation of free radical species and molecular products in water, so-called water radiolysis. The water radiolysis process occurs in three main stages taking place at different rates: physical (about 1 fs), physico-chemical ($10^{-15}$–$10^{-12}$ s), involving several processes, and chemical stage ($10^{-12}$–$10^{-6}$ s), with the formation of main products of water radiolysis (·OH, $e^-_{aq}$, ·H, $H_2$, $H_2O_2$, $H_3O^+$) (Trojanowicz 2020). The free radicals formed during water radiolysis are highly reactive; ·OH radicals are the most powerful oxidants known to occur in water, the same is valid for the hydrated electron and ·H radicals as reductants. These species result in the decomposition of various types of organic pollutants without radioactivity induction.

Based on the aforementioned traits, radiation technology is considered an effective and rapid method for wastewater treatment (Bojanowska-Czajka 2021). If the wastewater is resistant to biological treatment, ionizing radiation technology can be employed as a pretreatment to improve the biodegradability of wastewater. Besides, it can also be used as posttreatment for further advanced treatment of the effluent when the biological treatment process cannot meet the requirement of discharge standard, or the effluent needs to be reused (Wang et al. 2019). The application of gamma-rays for pollutant degradation has several advantages over conventional advanced oxidation processes because of the lack of chemical additives, the deeper penetration, the faster rate of radiolytic reaction, and being more effective and eco-friendly (Hina et al. 2021; Capodaglio 2020). In addition, the generation of oxidizing and reducing species simultaneously during water radiolysis has a beneficial role in the degradation different types of pollutants that can be removed through oxidation and/or reduction pathways (Hina et al. 2021; Kim et al. 2019).

Gamma irradiation has attracted considerable research attention for many years as an emerging technology that offers effective solutions for the degradation of MPs. Recently, more and more attention has been focused on the removal of MPs by ionizing radiation because of increasing awareness of the negative impact of these compounds on the natural environment. For instance, Trojanowicz et al. (2021) have expanded the earlier studies on $\gamma$-radiolytic decomposition of BPA in terms of comparing the radiolytic removal of BPA both in neutral aerated solutions and in solutions where the predominance of particular products of water radiolysis is ensured. Some recent studies reported that persulfate-based activation with ionizing radiation could enhance degradation and mineralization of MPs in a shorter period due to the formation of high amounts of reactive species (Senthilkumar et al. 2023; Zhang et al. 2020; Chu et al. 2019). Bezsenyi et al. (2020) have asserted that using gamma irradiation combined with cometabolic technology to remove persistent MPs could be successful and cost-effective. In addition, the first studies on the removal of different MPs by gamma irradiation have recently been reported by many researchers (Bujak et al. 2023; Ghazouani et al. 2022; Saadaoui et al. 2021; Chen and Wang 2020). However, most of the published work has focused on the effect of ionizing radiation on a single polluted solution and/or simulated (spiked with pollutants) wastewater. It is well known that in real life, contaminated water bodies are often polluted with a mixture of chemicals rather than a single chemical or chemical class. Therefore, the determination of the optimum irradiation dose for the removal of MPs is challenging because of the complexity and diversity of sample matrices. In real wastewater, there is competition between the pollutants and the matrix components for the reaction with the oxidizing and reducing species. This competition may have an impact on the overall efficiency of the treatment process. Such situations are dangerous because there is still very little knowledge about undesirable synergistic effects (Bojanowska-Czajka 2021). For this reason, this study is important as it is carried out with real wastewater effluent samples from a wastewater treatment plant in Kocaeli. Treatment of effluents by radiation technology has not been previously adopted for the treatment of wastewater in the study area.

MPs consist of a vast and expanding array of anthropogenic as well as natural substances. Particularly, nonsteroidal anti-inflammatory drugs (NSAIDs), estrogens, plasticizers, antimicrobial agents, synthetic surfactants, and amine-containing compounds are frequently detected in aquatic environments due to the widespread use of these chemicals (Luo et al. 2014). However, monitoring large numbers of MPs in water samples before and after the treatment process requires various analytical methods that are time-consuming, expensive, and resource-intensive. Therefore, 13 different MPs (ketoprofen, KET; diclofenac, DCF; ibuprofen, IBF; diethyl phthalate, DEP; bisphenol-A, BPA; triclosan, TCS; estrone, E1; 17-$\beta$-estradiol, E2; estriol, E3; 17-$\alpha$-ethinyl estradiol,

EE; diphenylamine, DPA; 4-octylphenol, 4-OP; 4-nonylphenol, 4-NP), being members of these groups and frequently detected, have been selected as target molecules to study their removal efficiency by ionizing radiation (Fig. S1). KET, DCF, and IBF are commonly used drugs due to their analgesic, antipyretic, and anti-inflammatory properties and are among the most frequently detected NSAIDs in aquatic systems around the world (Tyumina et al. 2020). DEP and BPA are frequently used in the plastic industry, as well as in medical devices, healthcare products, dispersants and emulsifying agents, epoxy resins, lubricants, auto parts, food packaging and services, paints, gelling agents, cosmetics, insecticides, and many other household and consumer products. These compounds have become major environmental concerns due to their genotoxicity, neurotoxicity, cytotoxicity, reproductive toxicity, and endocrine-disrupting effects, which may affect human health from gestation to adulthood (Dueñas-Moreno et al. 2022). Aside from these compounds, it has been reported that 4-NP and 4-OP are widely present in various mediums of the water environment as a result of photochemical or biological degradation of alkylphenol ethoxylates (commonly used nonionic surfactants). Therefore, the distribution of these chemicals in water environments and the ecological risk they pose are drawing broad attention (Dong et al. 2015). Recently, natural estrogens (E1, E2, E3, and EE) have become widespread in environmental water sources because traditional wastewater treatment processes could not completely remove them. Even at low concentrations (1 ng $L^{-1}$), they can interfere with the endocrine system of exposed organisms, resulting in abnormal expression of traits and reduced spawning rates (Ma et al. 2022). DPA has been widely used as a precursor of dyes, pesticides, pharmaceuticals, and photographic chemicals and as a stabilizer for explosives (Shin and Spain 2009; Drzyzga 2003). Owing to the high usage of DPA and its analogues, environmental contamination from these compounds has received increasing concern (Zhang et al. 2021b). TCS is a broad-spectrum antibacterial agent present as an active ingredient in some personal care products such as soaps, toothpastes, and sterilizers. It is an endocrine-disrupting compound, and its bioaccumulation in fatty tissues raises toxicity concerns (Olaniyan et al. 2016).

This study was conducted as a laboratory-scale investigation to provide a basis for future scale-up research regarding the radiation-induced treatment process of wastewater effluents. Therefore, real wastewater effluent samples were collected from a wastewater treatment plant, which will reflect the real concentration of target MPs and the treatment performance of gamma radiation. In this context, a validated analytical procedure (sample preparation and chromatographic analysis) was initially developed to simultaneously monitor target MPs in real samples both before and after irradiation. A vortex-assisted liquid–liquid extraction (VALLE) technique was optimized and used for the sample preparation stage. After the sample pre-concentration step, target MPs were analyzed using LC–ESI–MS. Then, the gamma irradiation process was applied to investigate the effect of ionizing radiation on the removal of target MPs from the effluent of the conventional wastewater treatment plant. The results of the research would provide useful information about strategies to treat the real micropollutant-containing wastewater with gamma radiation.

## Experimental

### Chemicals

The analytical standards of ketoprofen (≥ 98%), ibuprofen (≥ 98%), diethyl phthalate (99.5%), diclofenac sodium (≥ 98%), triclosan (97–103%), bisphenol-A (≥ 99%), 17-$\beta$-estradiol (≥ 98%), estriol (≥ 97%), 17-$\alpha$-ethinyl estradiol (≥ 98%), 4-nonylphenol (≥ 99.8%) were purchased from Sigma Aldrich. Diphenylamine (≥ 99.0%), 4-octylphenol (≥ 99.0%), and estrone (≥ 99.0%) were supplied by Merck, Alfa Aesar, and Acros Organics, respectively. The organic solvents methanol, acetonitrile, methyl tertiary-butyl ether, dichloromethane, dichloroethane, ethyl acetate, and chloroform were of HPLC grade. Acetic acid, hydrochloric acid, and ammonia were purchased from Merck. High-purity water was supplied by a Milli-Q Gradient Water Purification system (Millipore, Billerica, MA, USA).

Individual standard solutions of MPs (20 mg $L^{-1}$) were prepared in acetonitrile and used as stock standard solutions. Working standard solutions of target MPs were prepared by appropriate dilution of the stock solutions with the same solvent. Correspondingly, matrix-matched standards are prepared by adding standard solutions of MPs to the blank matrix obtained by the same extraction method procedure as for the samples (post-extraction spike method).

### Instrumentation and apparatus

Analyses were carried out using a HPLC system (Waters Alliance 2695 separations module; Waters, Milford, Massachusetts, USA) coupled to a single quadrupole mass spectrometer (Waters Micromass ZQ 2000, Manchester, UK). Chromatographic separation was performed on a XTerra® MS C18 (5 µm, 150 × 4.6 mm, Waters Milford, MA, USA) column. Several combinations of methanol, acetonitrile, purified water, and mobile-phase modifiers were investigated as mobile phases. The injection volume was set to 20.0 µL. The column and the autosampler were kept at 25 °C.

Selected MPs were ionized using electrospray ionization (ESI) in the positive and negative modes. The most intense ion peak at the optimum cone voltage of each analyte was

used for identification and quantification in the selected ion monitoring (SIM) mode. SIM detection was divided into time segments, and target analytes were recorded per segment. Other optimum mass spectrometric conditions are source temperature, 150 °C; desolvation temperature, 300 °C; capillary voltage, 3.5 kV; desolvation gas flow, 500 L $h^{-1}$ and cone gas flow, 50 L $h^{-1}$. Masslynx v4.1 software was used for data acquisition and processing.

The radiation treatment efficiency of the wastewater samples was also determined with respect to the changes in the pH, conductivity, and total organic carbon (TOC) values. A Mettler-Toledo SevenGo SG2 pH meter (Mettler-Toledo, Switzerland) connected with a Mettler-Toledo Inlab®413 pH electrode (Mettler-Toledo, Switzerland) was used to measure the pH of the samples. Calibration procedure was applied to probe of pH meter with standard buffer at 4.00 and 7.00. The conductivity measurements of the samples were carried out by a Mettler-Toledo SG3 conductivity meter (Mettler-Toledo, Switzerland) operating with an InLab®738 conductivity probe (Mettler-Toledo, Switzerland). Calibration procedure was applied to probe of electrical conductivity meter with potassium chloride standard buffer at 1413 µS/cm and 12.88 mS/cm. The pH and conductivity measurements were made in a thermostated water bath maintaining the temperature at 25 °C. TOC analyses were performed by using a TOC-TN analyzer (Hach-Lange IL 550 TOC, Hach-Lange, Germany) with a non-dispersive IR source, which was based on the combustion catalytic oxidation method. The color measurements were performed using a HACH-DR-890 colorimeter (Hach, Loveland, CO, USA) by following APHA platinum-cobalt standard method. The extracts were evaporated under reduced pressure using a rotary vacuum evaporator (Buchi Rotavapor R-210, Buchi, Switzerland) to dryness. Filtration of samples was accomplished using Millipore membrane filters (0.45 m Millipore Millex-HV membrane filter, Millipore, USA).

The gamma irradiation was carried out by using a $^{60}Co$ irradiator (Ob-Servo Sanguis, purchased from the Institute of Isotopes Co., Ltd., Budapest, Hungary) installed at Nuclear Energy Research Institute Ankara, Türkiye). Wastewater samples were irradiated at doses of 0, 10, 20, 30, and 50 kGy (dose rate: 1.35 kGy $h^{-1}$) at room temperature without any further treatment.

## Optimization of the extraction process

In the general procedure of the VALLE optimization studies, a 50-mL spiked sample solution was placed in a 250-mL volumetric flask. The extraction solvent was quickly transferred into the solution, and the MPs were extracted from the aqueous phase into the super-tiny drops of the extraction solvent through vortex agitation. Then, the emulsion was poured into a separatory funnel. After the two clear layers were formed, the organic phase was collected. The extracts were reduced to about 1 mL using a rotary evaporator, and then the rest of the solvent was evaporated to dryness at room temperature under a gentle stream of nitrogen. The residue was dissolved in 1 mL of acetonitrile (containing 0.5 mg $L^{-1}$ of each target compound) and analyzed by the optimized LC–ESI–MS method. By applying this procedure, parameters such as extraction solvent, volume ratio of organic/aqueous phase, pH, ionic strength, stirring speed, and stirring time were optimized. For each optimization step, one parameter was varied while the other parameters were held at a constant value. Triplicate extractions were carried out for each optimization step.

## Validation of the analytical procedure

Linearity, accuracy, precision, limit of detection (LOD), limit of quantification (LOQ), and matrix effect were determined to assess the performance of the method. The linearity for all target compounds was obtained by analyzing the standard solution in acetonitrile at twelve calibration levels.

LOD and LOQ were determined from the calibration curve method, as International Conference Harmonization (ICH) guideline recommendations (ICH 2005), and analyzed in three independent replicates of the calibration standards and calculated according to Eqs. (1) and (2):

$$\mathrm{LOD} = 3.3 \times (\sigma / S) \tag{1}$$

$$\mathrm{LOQ} = 10 \times (\sigma / S) \tag{2}$$

where $\sigma$ and $S$ are standard deviation of the intercept and slope of the calibration curve, respectively.

The matrix effect from sample preparation steps ($ME_{SPS}$) was estimated by comparing the slopes of solvent-matched standard curves (prepared using pure acetonitrile) and matrix-matched calibration curves (prepared using blank matrix extract). The matrix effect was calculated according to the following formula (Wang et al. 2017) (Eq. 3):

$$\mathrm{ME_{SPS}}(\%) = 100 \times [(\text{Slope of matrix matched} / \text{Slope of solvent matched}) - 1] \tag{3}$$

According to the literature (Wang et al. 2017; Kecojević et al. 2021), matrix effect is classified as mild or tolerable when ME (%) is less than ± 20%, medium when the value is between ± 20% and ± 50%, and strong when ME (%) is more than ± 50%.

The accuracy and precision of the whole analytical procedure (including extraction and LC–ESI–MS methods) were assessed by spike-recovery experiments. Blank samples were spiked with the target analytes at three concentration levels (0.05, 0.5, and 2.00 mg $L^{-1}$). The target compounds in

spiked samples were extracted, pre-concentrated, and analyzed by LC–ESI–MS using the optimized methods. The matrix-matched calibration standards were used to calculate the recoveries. The accuracy was expressed as the percentage recovery of the spiked samples. The precision was expressed as the %RSD of intraday (triplicates within the same day) and interday (triplicates for three consecutive days) repeatability.

## Analysis of real samples

The wastewater effluent samples were collected into glass bottles from Gebze wastewater treatment plant (Fig. 1) in Kocaeli and transferred to the laboratory. This plant is located at latitude 40.80557 and longitude 29.34997. The GPS coordinates are 40°48′20.1″N, 29°20′59.9″E.

All samples were stored in the dark at 4 °C. Color, TOC, pH, and conductivity were measured. For the extraction of target MPs, a 200 mL portion of the sample was transferred to a volumetric flask of 1 L. The pH of the sample was adjusted (if necessary), and extraction was performed according to the optimized parameters. After the organic phase separated, the extraction solvent was evaporated to dryness. The residue was then dissolved in 200 µL acetonitrile, conveyed to a glass micro-insert vial, and analyzed by the optimized LC–ESI–MS method. This procedure was carried out on three replicates. The target MPs were quantified with matrix-matched standards. $\%ME_{SMC}$ (matrix effect from the sample matrix components) was calculated using Eq. (4):

$$ME_{SMC}(\%) = 100 \times \left[ \frac{\left(A_{SS} - A_{USS} - A_{PWS}\right)}{A_{PWS}} \right] \tag{4}$$

where $A_{SS}$ is the peak area of the target compound determined in a real water sample extract post-spiked with the known concentration, $A_{USS}$ is the peak area of the target compound determined in the un-spiked water sample extract, and $A_{PWS}$ is the peak area of the target compound determined in the purified water extract post-spiked with the same concentration.

After the concentrations of MPs in wastewater effluent were determined, sample solutions were irradiated using a $^{60}Co$ gamma irradiation source with different doses (0–50 kGy). The samples were re-analyzed after irradiation to determine the color, TOC, pH, conductivity changes, and removal efficiencies. The removal efficiency was calculated based on the percent decrease in the level of MPs.

$$\text{Removal efficiency}(\%) = [(C_0 - C)/C_0] \times 100 \tag{5}$$

$C_0$ is the concentration of micropollutant before irradiation, $C$ is the concentration of micropollutant after irradiation.

The G-value is defined as the number of molecules formed or destroyed by absorbing 100 eV of energy. The chemical yield (removal efficiency of the pollutant) can be described by the G-value and is calculated on the basis of the following equation (Boujelbane et al. 2022; Woods and Pikaev 1994):

$$G\left(\mu \text{ mol } J^{-1}\right) = 10^6 \frac{\text{chemical yield}\left(\text{mol } L^{-1}\right)}{\text{Dose}(Gy)} \tag{6}$$

$G$ is the G-value, $D$ is the absorbed dose, and chemical yield is the change in concentration of the micropollutant (ΔC).

The dose constant, $k$, is the slope of the natural logarithm (ln) of the micropollutant concentration versus the absorbed dose (Boujelbane et al. 2022).

$$\ln\left(C/C_0\right) = -kD \tag{7}$$

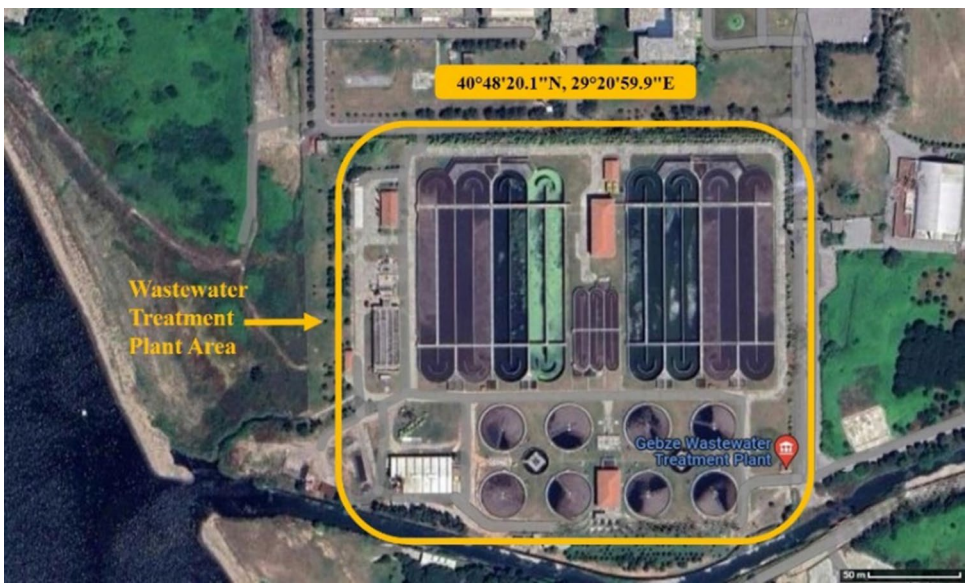


**Fig. 1** Sampling point on the google earth map

$C$ is the concentration of micropollutant after irradiation (mol $L^{-1}$), $C_0$ is the initial concentration of micropollutant (mol $L^{-1}$), k is the dose constant ($kGy^{-1}$) and $D$ is the absorbed dose (kGy).

Dose constants were used to calculate the absorbed doses required for 50% ($D_{0.5}$) and 90% ($D_{0.9}$) degradation of MPs by using the following equations, respectively (Boujelbane et al. 2022):

$$D_{0.5} = \ln 2/k \tag{8}$$

$$D_{0.9} = \ln 10/k \tag{9}$$

The data were expressed as means ± standard deviations. A one-way analysis of variance (ANOVA) ($\alpha = 0.05$) was performed among the mean values of the groups, and a $p$ value less than 0.05 was considered statistically significant.

## Results and discussion

### Optimization of LC–ESI–MS parameters

A C18 column (5 µm, 150 × 4.6 mm, Waters) that was suitable for the separation of the relatively polar target compounds was used in this study. In order to adjust the mobile-phase strength for a good separation of all analytes, the mixtures of water–methanol and water–acetonitrile, commonly used for ESI, were tested at different ratios using isocratic and gradient elution. Adding volatile weak organic acids and bases in low concentrations to the mobile phase can enhance the ESI ionization efficiencies of the compounds (Leito et al. 2008; Yang et al. 2012; Liigand et al. 2017). Therefore, the effect of acetic acid and ammonia as mobile-phase modifiers on the ESI response of target MPs was also investigated at final acid or base concentrations between 0.1 and 2% (v/v). The ESI–MS analyses were conducted in both positive and negative ion modes using cone voltages in the range of 20–60 V (in 5 V increments) to obtain the maximum ionization efficiency of each compound. The optimum values were selected based on the highest MS signal obtained.

Optimization studies showed that the best method for the analysis of the selected MPs was achieved using two different instrumental conditions. The LC–ESI–MS Method 1 (M1) was developed for KET, DEP, DCF, and DPA (Group 1) using acetonitrile (A) and water containing 2% acetic acid (B) mixtures with a gradient elution program in the ESI positive mode. The LC–ESI–MS Method 2 (M2) was developed with a gradient program using acetonitrile (A) and water containing 0.5% ammonia (B) mixtures for IBF, BPA, TCS, E1, E2, E3, EE, 4-OP, and 4-NP (Group 2) in the ESI negative mode. The detailed liquid chromatographic and mass spectrometric operating parameters for the determination of target MPs are presented in Table 1. The representative total ion chromatograms of target analytes in SIM mode of multi-channel and single-channel are shown in Figs. S2, S4 and Figs. S3, S5, respectively.

### Optimization of the extraction process

In the preliminary studies, the VALLE method provided higher recoveries and lower standard deviations than SPE for the samples containing all target analytes. The parameters that impact the extraction efficiency were optimized as detailed below.

#### Selection of extraction solvent for VALLE

A crucial step in method optimization for liquid–liquid extraction is the selection of the most suitable organic solvent to be employed. The solvent has to form a cloudy state that increases the contact area between the two phases to provide high extraction efficiency (Psillakis and Kalogerakis 2003). For this purpose, methyl tertiary-butyl ether (MTBE), dichloromethane (DCM), ethyl acetate (EA), chloroform (CHL), and dichloroethane (DCE) were evaluated in this study.

Among the solvents examined in this study, DCM was found to be the most suitable for the extraction of Group 1, according to the recovery results presented in Fig. 2a and Table S1. As seen in Fig. 2b and Table S1, all tested solvents exhibited high extraction yields for BPA, E2, EE, E1, 4-OP, and 4-NP. In the case of E3, however, none of them produced satisfactory recovery results (< 41%). One possible explanation for this finding would be its greater ability to form hydrogen bonds with water molecules because of its three hydroxy groups. The H-bonded clusters of E1, E2, and E3 with a water molecule have been investigated using various laser spectroscopic methods and quantum chemical calculations by Morishima et al. (2013). The authors reported the hydrogen bonding ability of three hydroxy groups (one phenolic OH and two alcoholic OH) of E3 and the formation of a stable ring-structure hydrogen bonding network between two alcoholic OH groups and water. The ability of E3 to form stable hydrogen bonds could possibly play a key role in the low solubility of this molecule in the organic phase and hence its low extraction efficiency. In these circumstances, IBF and TCS were the micropollutants that specified the extraction solvent for Group 2. The best recoveries for these molecules were obtained in MTBE. Therefore, DCM for Group 1 and MTBE for Group 2 were selected as the extraction solvents in further studies.

**Table 1** LC and MS operating parameters for target MPs

| MPs | LC (M1)** | | | | MS (M1)** | | | |
|---|---|---|---|---|---|---|---|---|
| G1* | Time(min) | Flow (mL/min) | $CH_3CN$(%) | 2% $CH_3COOH$(%) | Ion source | Cone voltage(V) | Base peak | TS***(min) |
| KET | 00.00 | 1 | 60 | 40 | ESI+ | 25 | 254.84 | 2.50–3.25 |
| DEP | 07.00 | 1 | 50 | 50 | ESI+ | 15 | 222.77 | 3.30–4.40 |
| DCF | 08.00 | 1 | 60 | 40 | ESI+ | 35 | 249.73 | 4.12–5.18 |
| DPA | | | | | ESI+ | 40 | 169.78 | 5.60–7.00 |
| MPs | LC (M2)** | | | | MS (M2)** | | | |
| G2* | Time(min) | Flow (mL/min) | $CH_3CN$(%) | 0.5% $NH_3$(%) | Ion source | Cone voltage(V) | Base peak | TS***(min) |
| IBF | 00.00 | 0.20 | 50 | 50 | ESI- | 10 | 204.80 | 2.80–4.50 |
| TCS | 12.00 | 0.50 | 70 | 30 | ESI- | 10 | 286.90 | 3.50–7.00 |
| E3 | 30.00 | 0.50 | 100 | 0 | ESI- | 50 | 286.91 | 4.80–7.00 |
| BPA | 31.00 | 0.50 | 50 | 50 | ESI- | 30 | 226.80 | 7.00–9.00 |
| E2 | 32.00 | 0.20 | 50 | 50 | ESI- | 50 | 270.84 | 9.00–10.10 |
| EE | 33.00 | 0.20 | 50 | 50 | ESI- | 50 | 294.85 | 9.00–11.00 |
| E1 | | | | | ESI- | 50 | 268.83 | 9.50–12.00 |
| 4-OP | | | | | ESI- | 35 | 204.81 | 20.80–24.00 |
| 4-NP | | | | | ESI- | 35 | 218.86 | 23.00–27.00 |

* *G*1 group 1, *G*2 group 2

** *M*1 method 1, *M*2 method 2

*** *TS* time segment

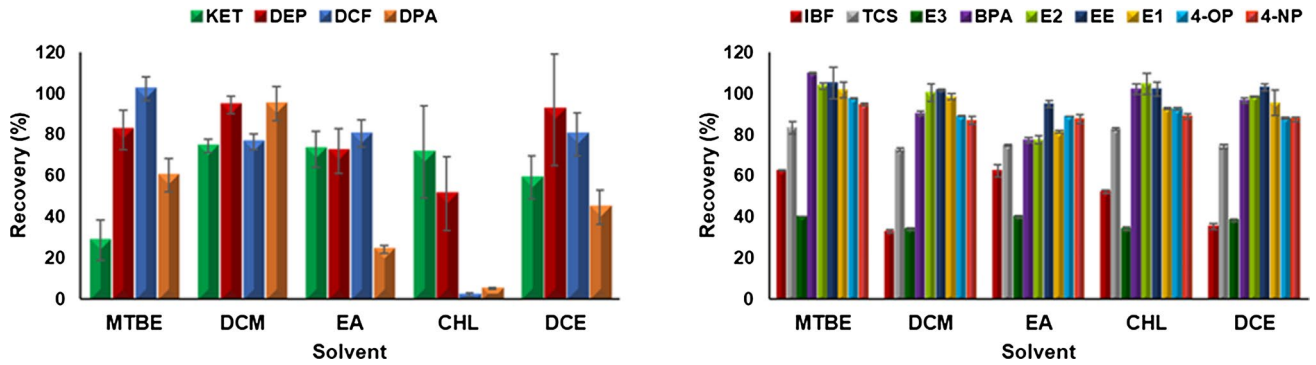


**Fig. 2** Effect of solvent type on the recovery of target **a** Group 1, **b** Group 2 MPs. Other experimental conditions: organic to aqueous phase ratio (O/A), 1:1; pH of the aqueous phase, 7; no salt addition; stirring speed, 2000 rpm; stirring time, 10 min

### Effect of volume of extraction solvent

The extraction solvent volume also plays a significant role in the extraction efficiency of the VALLE process. The effect of different O/A (1:1, 1:2, 1:5, and 1:10) on the extraction efficiencies of the target analytes is presented in Fig. 3 and Table S2.

The maximum recoveries of all Group 1 analytes were observed at a ratio of 1:1 (> 74%) and decreased to < 45% at a 1:10 ratio, as illustrated in Fig. 3a and Table S2. On the other hand, the extraction efficiency of Group 2 MPs did not change significantly with the reduction of the volume fraction of MTBE (Fig. 3b and Table S2), When two immiscible liquids are subjected to a turbulent flow (which was carried out using a magnetic stirrer in this study), an emulsion is formed as a result of drop interactions with eddies. More stress (agitation) is required to generate microdroplets for the two immiscible liquids with high interfacial tension values (Psillakis 2019; Shahid et al. 2017; Tadros et al. 2004). It has been reported that interfacial tension value of water-DCM system (~ 28 mN/m) (Pisani et al. 2008) is higher than water-MTBE system (~ 9 mN/m) (Cárdenas et al. 2015). As

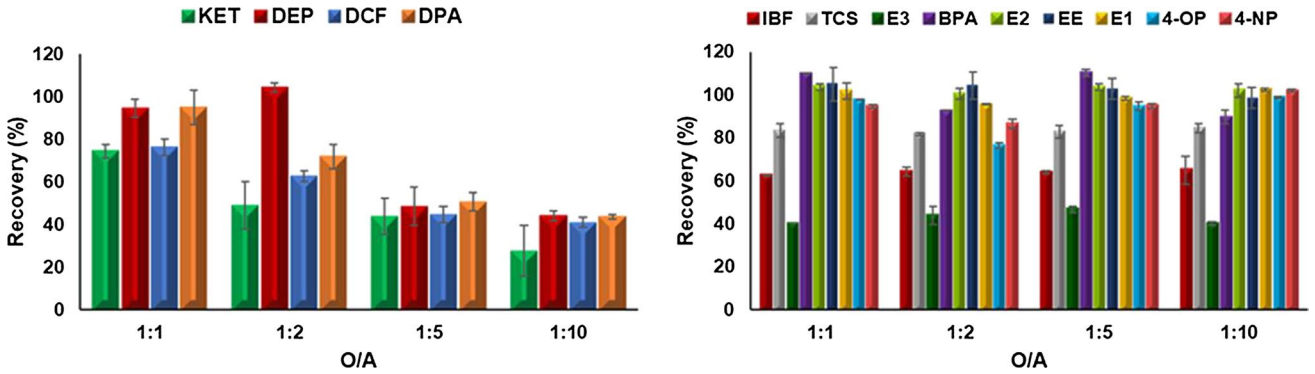


**Fig. 3** Effect of volume of extraction solvent on the recovery of target **a** Group 1, **b** Group 2 MPs. Other experimental conditions: extraction solvent, DCM for Group 1, MTBE for Group 2; pH of the aqueous phase, 7; no salt addition; stirring speed, 2000 rpm; stirring time, 10 min

mentioned, the stirring speed of 2000 rpm was kept constant at all O/A ratios for both systems in this study. Therefore, it could be suggested that microdroplets generated at this stirring speed were more in the water-MTBE system than in the water-DCM system at the same O/A ratio. In this context, while a low MTBE/water ratio (1:10) was sufficient for the effective mass transfer of Group 2 analytes, the number of microdroplets formed at the same DCM/water ratio (1:10) was not enough to extract the Group 1 analytes completely with a single-stage extraction. As a result, extraction efficiencies for Group 1 analytes decreased with a decreasing volume ratio of DCM. Therefore, an O/A of 1:1 was selected as the optimum ratio and used for the extraction of Group 1 compounds in the further experiments. Since the extraction efficiency of Group 2 MPs did not change significantly with the volume ratio change of the phases, an O/A of 1:10 was used in subsequent extractions of Group 2 analytes to reduce solvent consumption and minimize the negative environmental impact of waste.

### Effect of ionic strength

Depending on the nature of the target analytes, an increase in the ionic strength of the aqueous phase can enhance (salting-out effect), not influence, or decrease (salting-in effect) their solubility (Psillakis and Kalogerakis 2003). In this context, different concentrations of NaCl in the range of 0–10% (w/v) were studied to investigate the effect of salt addition on the extraction recovery of target MPs.

The results showed that the percentage extraction yield of KET, DCF, and IBF did not change significantly within the NaCl range of 0–1% but decreased when the concentration of NaCl in the aqueous phase increased above 1% (salting-in effect) (Fig. 4 and Table S3). Under these conditions, the electrostatic interaction between the anionic forms of KET, DCF, and IBF with salt ions in the neutral solution may have reduced their ability to move into the organic phase (Lord and Pawliszyn 2000). On the other hand, the addition of NaCl had no significant effect on the extraction recovery of DEP, DPA, E1, E2, EE, 4-OP, and 4-NP (Fig. 4 and

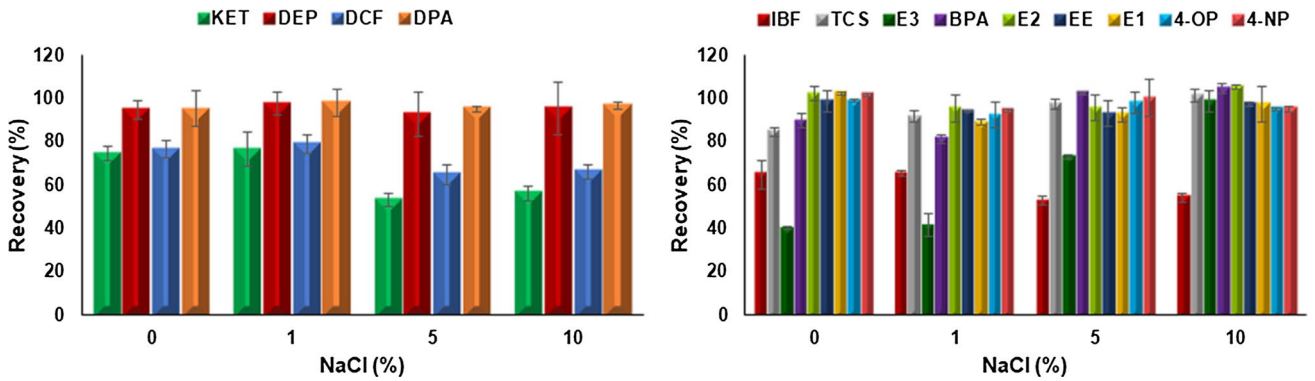


**Fig. 4** Effect of ionic strength on the recovery of target **a** Group 1, **b** Group 2 MPs. Other experimental conditions: extraction solvent, DCM for Group 1, MTBE for Group 2; O/A, 1:1 for Group 1, 1:10 for Group 2; pH of the aqueous phase, 7; stirring speed, 2000 rpm; stirring time, 10 min

Table S3). In the case of TCS, BPA, and E3, the addition of salt in the 5–10% range led to an increase in the extraction yield via the salting-out effect. As a consequence, salt addition was not used in the extraction of Group 1 in the subsequent experiments. Since the addition of salt provided a pronounced increase, particularly in the extraction yield of E3, further extractions for Group 2 were carried out at a NaCl concentration of 10%.

Wastewater samples can naturally have a certain ionic strength background due to the presence of ionic species. Thus, the level of ionic strength in these samples can change the extraction efficiency of target MPs, particularly KET, DCF, and IBF, as mentioned above. Therefore, the findings have also been evaluated in terms of conductivity values, which represent the ionic strength of water samples. The conductivities of 0, 1, 5, and 10% NaCl solutions spiked with 0.5 mg $L^{-1}$ of target MPs were found to be 0.0011, 20.57, 76.30, and 132.30 mS $cm^{-1}$, respectively. These data indicated that conductivity values up to 21 mS $cm^{-1}$ had no effect on the extraction efficiencies of target MPs. The extraction efficiencies of KET, DCF, and IBF, on the other hand, decreased with increasing conductivity, in other words, ionic strength, and remained almost constant at higher ionic strength values ($\gtrsim$ 76 mS $cm^{-1}$). Adjusting the solution pH to the acidic region, which converts all KET, DCF, and IBF species to uncharged forms, can compensate for the negative impact of ionic strength on their extraction efficiencies. This approach is examined in the next section.

### Effect of pH

The pH of the sample solution is an important parameter that has a significant impact on the extraction of analytes (especially acid–base species) from water samples (Rahimi-Nasrabadi et al. 2012). Since most of the target compounds in this study (TCS, BPA, E1, E2, E3, EE, 4-OP, and 4-NP) have high pKa values (pKa ≥ 8), their dissociated forms predominate under alkaline conditions, making them more soluble in water than organic solvents. Considering this, the effect of sample pH on extraction efficiency was investigated under neutral and acidic conditions.

As can be seen clearly in Fig. 5 and Table S4, the extraction recoveries of KET, DCF, and IBF increased as the pH of the solution decreased from 7 to 3.5, with pH 3.5 yielding the highest extraction efficiency. KET, DCF, and IBF have low pKa values (pKa < 5); therefore, the anionic forms of these compounds are expected to be the major species at higher pH values, while the non-ionized species, which can easily be extracted into the organic extraction solvent, predominate at lower pH.

Since DEP, TCS, BPA, E1, E2, E3, EE, 4-OP, and 4-NP do not have a clearly noticeable acid–base property, only a slight decrease in the recovery of this molecule was observed when the pH of the solution was decreased from 7 to 3.5. On the other hand, the reduction in the extraction efficiency of DPA was much more pronounced under these conditions. DPA is an alkaline insoluble molecule at high pH, and at low pH it forms a salt (Ma et al. 2021). Accordingly, at low pH values, the solubility of DPA in the water phase increased due to salt formation; therefore, low extraction recoveries were obtained. When the pH was neutral, it existed in molecular form that could be easily extracted by the organic phase with a high extraction efficiency. In light of these findings, subsequent extractions of all target MPs were carried out at two pH values (neutral and 3.5) to achieve the best extraction efficiency.

### Effect of stirring speed and time

As liquid–liquid extraction is a mass-transfer process, creating fine droplets with the assistance of a vortex agitator

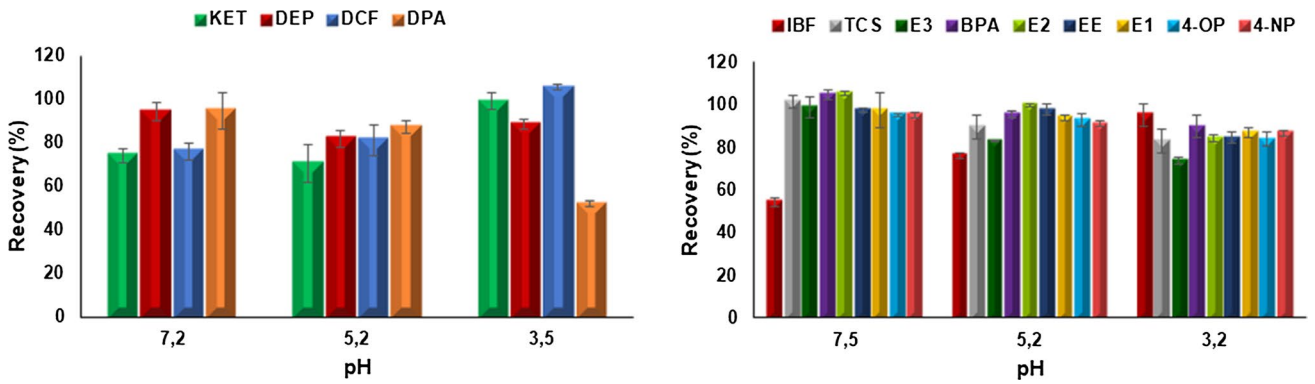


**Fig. 5** Effect of pH on the recovery of target **a** Group 1, **b** Group 2 MPs. Other experimental conditions: extraction solvent, DCM for Group 1, MTBE for Group 2; O/A, 1:1 for Group 1, 1:10 for Group 2; no salt addition for Group 1, 10% NaCl addition for Group 2; stirring speed, 2000 rpm; stirring time, 10 min

system enhances the interfacial area available for mass transfer, reduces the diffusion distance, and improves the extraction rates (Psillakis 2019). At this point, stirring speed and time are the parameters that influence the formation of a cloudy solution consisting of fine droplets and therefore need to be optimized. In this regard, the effects of stirring speed and time on the extraction of MPs were examined in the ranges of 0–2000 rpm and 0–15 min, respectively. Stirring speed investigations were performed at the indicated rpms with 10 min of stirring. The "0 rpm" point represented the extraction where the water–organic mixture was not subjected to stirring and the target chemicals were extracted by diffusion for 10 min. In stirring time experiments, the stirring speed of the magnetic stirrer was kept constant at 2000 rpm (the maximum setting value).

The results indicated that the extraction yields of all compounds increased gradually as the stirring speed increased and reached their highest values at 2000 rpm (Fig. 6 and Table S5). This increase can be explained by the efficient dispersion of the extraction solvent in the aqueous phase and the formation of a stable cloudy solution. Initially, large drops of solvent are present in the aqueous phase. As the process of agitation proceeds, these drops are deformed and further broken down into smaller and smaller ones. At high rotational speeds, the size of droplets is very small, leading to an increase in the contact area available for mass transfer (Psillakis 2019). Due to the limitations of our magnetic stirrer, a stirring speed of more than 2000 rpm could not be investigated. After determining that 2000 rpm was the best stirring speed, the extraction procedure was carried out at several stirring times. According to the findings, the extraction efficiency increased with stirring time up to 10 min and then remained nearly constant for all target MPs (Fig. 7 and Table S6). This finding indicated that the mass-transfer equilibrium was obtained within 10 min of agitation for all target MPs. Hence, a stirring speed of 2000 rpm for 10 min was used for the subsequent experiments.

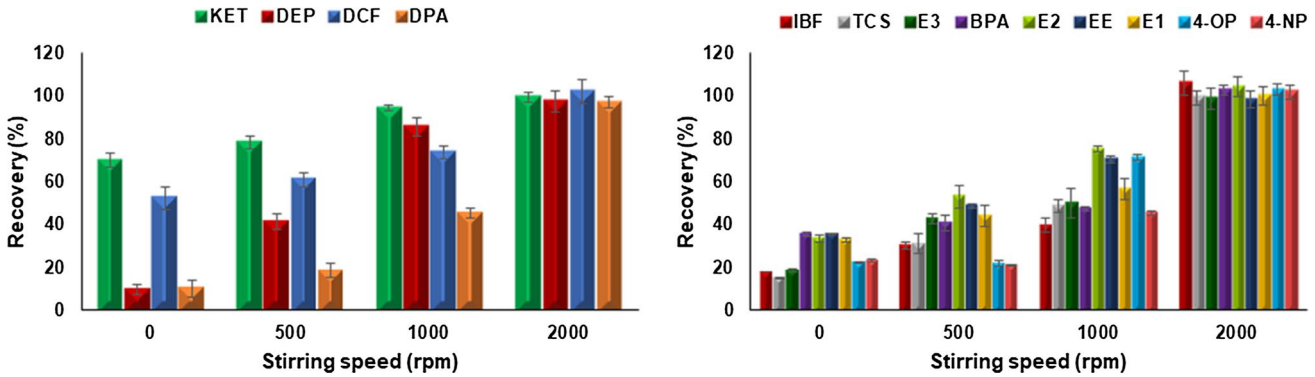


**Fig. 6** Effect of stirring speed on the recovery of target **a** Group 1, **b** Group 2 MPs. Other experimental conditions: extraction solvent, DCM for Group 1, MTBE for Group 2; O/A, 1:1 for Group 1, 1:10 for Group 2; no salt addition for Group 1, 10% NaCl addition for Group 2; pH of the aqueous phase, 7 for the first extraction, 3.5 for the second extraction; stirring time, 10 min

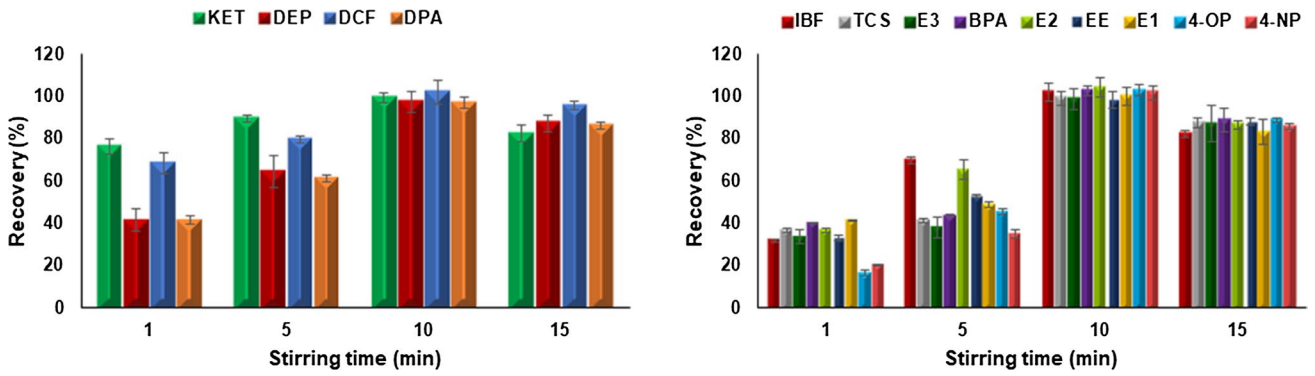


**Fig. 7** Effect of stirring time on the recovery of target **a** Group 1, **b** Group 2 MPs. Other experimental conditions: extraction solvent, DCM for Group 1, MTBE for Group 2; O/A, 1:1 for Group 1, 1:10 for Group 2; no salt addition for Group 1, 10% NaCl addition for Group 2; pH of the aqueous phase, 7 for the first extraction, 3.5 for the second extraction; stirring speed, 2000 rpm

In light of the studies mentioned above, a brief overview of the optimized analytical procedure for the analysis of 13 MPs is given in Scheme S1.

## Validation of the analytical procedure

The major goal of the validation is to demonstrate that the proposed procedure meets the requirements for the intended analytical applications. Therefore, typical validation characteristics such as linearity, LOD, LOQ, accuracy, and precision were assessed.

As the instrumental LOD and LOQ were at the μg $L^{-1}$ levels (Table 2), a pre-concentration factor of up to 1000-fold was required for the determination of MPs at the ng $L^{-1}$ level. The matrix effect that may arise from the sample preparation procedure and high pre-concentration processes was evaluated by using ultrapure water as a blank matrix. The blank matrix samples were treated as described in Scheme S1, pre-concentrated 1000-fold, and then spiked with different concentrations of target MPs in order to obtain matrix-matched standards (post-extraction spike method). The slope of the calibration curve for these matrix-matched standard solutions was compared with that of solvent-matched standard solutions according to Eq. (3).

According to the results obtained, soft signal suppression was found for KET (−19.15%), DEP (−7.89%), DPA (−8.47%), TCS (−6.07%), 4-OP (−2.80%), and 4-NP (−4.28%), while the signal suppression was more pronounced for DCF (-30.77%). On the other hand, sample preparation and the subsequent pre-concentration procedure gave rise to a mild signal enhancement for E3 (11.11%) and EE (8.46%) and a moderate signal enhancement for BPA (20.29%), E2 (26.87%), and E1 (21.48%). Due to the negative impact of matrix on the analyte response, the accuracy and precision of the entire analytical procedure (from extraction to analysis, Scheme S1) were assessed at three concentration levels (0.05, 0.5, and 2.0 μg $mL^{-1}$) using matrix-matched standards.

As shown in Table S7, the mean recoveries of 13 MPs obtained using matrix-matched standards varied from 94 to 109%. The RSDs for intraday ($RSD_r$) and interday ($RSD_R$) precision were in the range of 0.11–4.90% and 1.73–8.78%, respectively. Good recoveries and RSDs indicate that the proposed extraction and LC–ESI–MS methods provide high accuracy and precision.

**Table 3** Average concentrations of target MPs and matrix effect in wastewater effluent

| Wastewater effluent | | | | |
|---|---|---|---|---|
| MPs | Wastewater μg $L^{-1}$ | Spiked μg $L^{-1}$ | Found μg $L^{-1}$ | $ME_{SMC}$[2](%) |
| KET | 0.943 ± 0.088 | 0.5 | 1.403 ± 0.068 | −6.84 |
| DEP | 0.564 ± 0.015 | 0.5 | 1.167 ± 0.113 | 12.64 |
| DCF | 0.227 ± 0.021 | 0.1 | 0.342 ± 0.014 | 6.62 |
| DPA | 0.019 ± 0.004 | 0.01 | 0.025 ± 0.004 | −12.09 |
| IBF | 0.304 ± 0.041 | 0.5 | 0.791 ± 0.032 | −4.01 |
| TCS | 0.567 ± 0.017 | 0.5 | 1.061 ± 0.012 | −6.26 |
| E3 | ND[1] | 0.05 | 0.046 ± 0.005 | −3.59 |
| BPA | 0.578 ± 0.042 | 0.5 | 1.072 ± 0.031 | −1.70 |
| E2 | 0.006 ± 0.002 | 0.01 | 0.015 ± 0.005 | −8.49 |
| EE | ND[1] | 0.05 | 0.045 ± 0.005 | −5.02 |
| E1 | 0.008 ± 0.002 | 0.01 | 0.016 ± 0.003 | −7.01 |
| 4-OP | 0.005 ± 0.002 | 0.01 | 0.015 ± 0.003 | −3.67 |
| 4-NP | ND[1] | 0.05 | 0.046 ± 0.003 | −3.12 |

**Table 2** Instrumental linear range, LOD, and LOQ for the determination of the target MPs

| MPs | Linear range (μg $L^{-1}$) | Correlation coefficient | SD of the intercept($\sigma$) | Slope($S$) | LOD(μg $L^{-1}$) | LOQ(μg $L^{-1}$) |
|---|---|---|---|---|---|---|
| KET | 2.61–3.0 × $10^3$ | 0.9994 | 58.56 | 224,575 | 0.86 | 2.61 |
| DEP | 4.30–3.0 × $10^3$ | 0.9995 | 106.25 | 246,565 | 1.42 | 4.30 |
| DCF | 2.75–3.0 × $10^3$ | 0.9997 | 32.25 | 117,247 | 0.91 | 2.75 |
| DPA | 3.34–3.0 × $10^3$ | 0.9994 | 81.41 | 243,928 | 1.10 | 3.34 |
| IBF | 2.79–3.0 × $10^3$ | 0.9997 | 37.83 | 135,454 | 0.92 | 2.79 |
| TCS | 12.69–3.0 × $10^3$ | 0.9996 | 3.89 | 3063 | 4.19 | 12.69 |
| E3 | 3.60–3.0 × $10^3$ | 0.9996 | 26.49 | 73,515 | 1.19 | 3.60 |
| BPA | 3.04–3.0 × $10^3$ | 0.9998 | 74.30 | 71,234 | 1.01 | 3.04 |
| E2 | 3.31–3.0 × $10^3$ | 0.9996 | 51.62 | 52,592 | 1.09 | 3.31 |
| EE | 30.10–3.0 × $10^3$ | 0.9995 | 77.23 | 41,284 | 9.92 | 30.10 |
| E1 | 3.10–3.0 × $10^3$ | 0.9997 | 60.10 | 66,826 | 1.02 | 3.10 |
| 4-OP | 2.56–3.0 × $10^3$ | 0.9998 | 31.45 | 123,017 | 0.84 | 2.56 |
| 4-NP | 6.49–3.0 × $10^3$ | 0.9995 | 125.16 | 192,885 | 2.14 | 6.49 |

## Analysis of real samples

The proposed method was used to determine the concentrations of target MPs in wastewater effluent samples (Table 3). As can be seen in Table 3, with the exception of E3, EE, and 4-NP, the concentrations of all target MPs in wastewater effluent were found to be above the method detection limits. These findings confirm that conventional wastewater treatment is insufficient to remove all pollutants from wastewater.

As mentioned previously, the matrix effect arising from the sample extraction and high pre-concentration processes was compensated for by matrix-matched calibration. Besides, the matrix components of wastewater effluent samples may have caused the suppression or enhancement of analyte ionization, leading to quantification errors. Furthermore, co-eluting components may have produced similar ions in MS experiments, which leads to a false interpretation of results, especially when these components are present in high concentrations in the extract and eluted in the same retention window as the target compounds (Caban et al. 2012). Therefore, the accuracy of the results was determined by spiking with known concentrations of the analytes and calculating the matrix effect using Eq. 4.

It was found that the increase and decrease in signal intensities of all target MPs, except DEP, DCF, and TCS, were within the standard deviation of the mean values, indicating that matrix components in the wastewater samples did not exhibit a matrix effect. However, the matrix components of the wastewater effluent sample showed a soft enhancement in the DEP (12.64%) and DCF (6.62%) signals, whereas a soft suppression in the TCS (−6.26%) signal.

These findings confirmed that our method yields accurate results and that the optimized analytical procedure can be used to investigate the effect of ionizing radiation on target MPs in wastewater effluent.

## Effect of gamma irradiation on target MPs

Processes based on high-energy electromagnetic radiation are more economical and effective on a large scale than other techniques used to remove persistent pollutants from waters and wastewaters (Rivera-Utrilla et al. 2013). In this study, to investigate the effectiveness of ionizing radiation in treating MPs in wastewater effluents, real samples obtained from the wastewater treatment plant were irradiated at several doses ranging from 0 to 50 kGy.

Table 4 shows the change in color, pH, conductivity, and TOC. As illustrated in Table 4, gamma irradiation treatment significantly removed the color of wastewater effluent (46% at 10 kGy and 100% at 20 kGy). The color reduction is mainly due to the decomposition of colored organic compounds in the wastewater effluent. The pH of the samples showed a decrease when a dose of 10 kGy was applied. However, no significant difference in pH values was detected between the samples irradiated at 10 and 20 kGy ($p = 0.05$). On the other hand, the influence of 30 kGy gamma doses on the pH value was significant, whereas there was no statistically significant difference in pH between the samples irradiated at 30 and 50 kGy ($p = 0.10$). The reduction in pH can be explained by the conversion of organic compounds in the wastewater sample to lower-weight organic acids by reacting with oxidizing species (Hina et al. 2021). At dose values where no difference in pH is observed, the by-products may have no noticeable acidic character, or the decomposition process of some pollutants may be completed. When a dose of 30 kGy was applied, the more resistant compounds may have begun to decompose. Conductivity measurements were used to monitor the radiation-induced changes in the ionic strength of the wastewater. Irradiation could cause changes in total salt concentration due to the degradation process and thus change conductivity. This change could affect the extraction efficiency, as mentioned previously. According to the results obtained, the conductivity values showed no significant change with the irradiation doses ($p = 0.08$). In addition, the conductivity values are not at a level ($< 21$ mS cm$^{-1}$) that will affect the extraction yield of the samples. TOC was monitored to determine the efficiency of the radiation-induced treatment process. The TOC value gradually decreased with an increase in the irradiation dose, indicating the decomposition of target MPs and other organic matrix components.

After gamma irradiation at a dose of 10 kGy, E1, E2, and 4-OP were not detected in irradiated wastewater samples (Table 5). The concentration of other target

**Table 4** Effect of different irradiation doses on the color, pH, electrical conductivity (EC), and total organic carbon (TOC) values of wastewater effluent

| Dose (kGy) | Color | Color Change% | pH | pH Change% | EC (mS/cm) | EC Change% | TOC (mg/L) | TOC Change% |
|---|---|---|---|---|---|---|---|---|
| 0 | 13 | – | 7.12 | – | 1.99 | – | 6.22 | – |
| 10 | 7 | 46.15% | 7.01 | 1.55% | 2.02 | 1.51% | 4.82 | 22.43% |
| 20 | 0 | 100% | 6.98 | 1.97% | 2.03 | 2.01% | 4.03 | 35.23% |
| 30 | 0 | 100% | 6.75 | 5.19% | 2.03 | 2.01% | 3.57 | 42.53% |
| 50 | 0 | 100% | 6.78 | 4.78% | 2.01 | 1.00% | 3.31 | 46.78% |

**Table 5** Variation of the target MPs concentration, removal efficiency, and G-values, with the absorbed doses, $D_{0.5}$ and $D_{0.9}$ values

| Wastewater effluent | | | | | | |
|---|---|---|---|---|---|---|
| MPs | Irradiation dose | Concentration | Removal efficiency | G-value | $D_{0.5}$ | $D_{0.9}$ |
| | kGy | μg $L^{-1}$ | % | μmol $J^{-1}$ | kGy | kGy |
| KET | 0 | 0.943 ± 0.088 | – | – | 13.75 | 45.69 |
| | 10 | 0.520 ± 0.016 | 44.86 | 0.166 | | |
| | 20 | 0.343 ± 0.039 | 63.58 | 0.118 | | |
| | 30 | 0.202 ± 0.008 | 78.58 | 0.097 | | |
| | 50 | 0.192 ± 0.011 | 79.64 | 0.059 | | |
| DEP | 0 | 0.564 ± 0.015 | – | – | 12.14 | 40.32 |
| | 10 | 0.264 ± 0.036 | 53.19 | 0.135 | | |
| | 20 | 0.182 ± 0.036 | 67.73 | 0.086 | | |
| | 30 | 0.095 ± 0.014 | 83.16 | 0.070 | | |
| | 50 | 0.103 ± 0.006 | 81.74 | 0.042 | | |
| DCF | 0 | 0.227 ± 0.021 | – | – | 5.10 | 16.96 |
| | 10 | 0.053 ± 0.010 | 76.65 | 0.059 | | |
| | 20 | 0.015 ± 0.005 | 93.39 | 0.036 | | |
| | 30 | 0.011 ± 0.001 | 95.15 | 0.024 | | |
| | 50 | 0.013 ± 0.003 | 94.27 | 0.014 | | |
| DPA | 0 | 0.019 ± 0.004 | – | – | 8.90 | 29.56 |
| | 10 | 0.008 ± 0.002 | 57.89 | 0.006 | | |
| | 20 | 0.004 ± 0.001 | 78.94 | 0.005 | | |
| | 30 | ND | – | – | | |
| IBF | 0 | 0.304 ± 0.041 | – | – | 3.51 | 11.67 |
| | 10 | 0.042 ± 0.003 | 86.18 | 0.127 | | |
| | 20 | 0.044 ± 0.003 | 85.53 | 0.063 | | |
| | 30 | 0.043 ± 0.002 | 85.86 | 0.042 | | |
| | 50 | 0.043 ± 0.004 | 85.86 | 0.025 | | |
| TCS | 0 | 0.567 ± 0.017 | – | – | 3.16 | 10.49 |
| | 10 | 0.062 ± 0.006 | 89.07 | 0.174 | | |
| | 20 | 0.007 ± 0.003 | 98.77 | 0.097 | | |
| | 30 | 0.011 ± 0.003 | 98.06 | 0.064 | | |
| | 50 | 0.009 ± 0.004 | 98.41 | 0.038 | | |
| BPA | 0 | 0.578 ± 0.042 | – | – | 3.93 | 13.07 |
| | 10 | 0.080 ± 0.004 | 86.16 | 0.218 | | |
| | 20 | 0.017 ± 0.004 | 97.06 | 0.122 | | |
| | 30 | 0.012 ± 0.003 | 97.92 | 0.083 | | |
| | 50 | 0.014 ± 0.003 | 97.58 | 0.049 | | |
| E2 | 0 | 0.006 ± 0.002 | – | – | – | – |
| | 10 | ND | – | – | – | – |
| E1 | 0 | 0.008 ± 0.002 | – | – | – | – |
| | 10 | ND | – | – | – | – |
| 4–OP | 0 | 0.005 ± 0.002 | – | – | – | – |
| | 10 | ND | – | – | – | – |

MPs drastically decreased with the increased dose up to 10 kGy for IBF, 20 kGy for DCF, DPA, TCS, and BPA, and 30 kGy for KET and DEP (Table 5). No significant differences were detected between the concentrations of IBF irradiated at 10, 20, 30, and 50 kGy doses ($p = 0.86$). Similarly, there is no significant difference between the concentrations of DCF ($p = 0.19$), TCS ($p = 0.56$), and BPA ($p = 0.43$) in the samples irradiated at 20, 30, and 50 kGy. In addition, no significant difference is found

between the concentrations of KET ($p = 0.36$) and DEP ($p = 0.27$) in irradiated samples at 30 and 50 kGy.

The idea of employing ionizing radiation to decompose pollutants in the aqueous phase is based on the assumption that any emitted radiation is characterized by its ability to accumulate its energy in the surrounding medium, which is water (Bojanowska-Czajka 2021). When gamma irradiation reacts with water, a chain reaction occurs, and reactive species responsible for oxidation and reduction are formed. The radiolysis of water and the main active species formed can be presented as:

$$H_2O \rightarrow e_{aq}^-, \bullet OH, \bullet H, H_2, H_2O_2, H_3O^+$$

In water radiolysis, hydroxyl radicals (·OH) as powerful oxidants and solvated electrons ($e_{aq}^-$) and hydrogen radicals (·H) as strong reducing agents are main reactive species for degrading contaminants. $H_2O_2$ and $H_2$ have limited contribution to the decomposition of target compounds due to their low yield and reactivity (Alsager et al. 2018). It is noteworthy that these species are produced simultaneously by ionizing radiation (Woods and Pikaev 1994). This is different from commonly used AOPs such as ozonation and Fenton oxidation, which means organic contaminants would react not only with oxidizing species but also with reducing radicals (Chu and Wang 2016). ·OH radicals behave as electrophiles, while $e_{aq}^-$ act as nucleophiles in the reaction with organic substances (Wang and Chu 2016). However, each reaction mechanism depends on the molecular structures and functional groups present in the target molecules. For instance, the radiation-induced degradation of DCF was reported to take place via reduction by $e_{aq}^-$ and oxidation by ·OH radicals (Homlok et al. 2011). On the other hand, it was reported that ·OH is more effective in decomposing KET than $e_{aq}^-$ (Illés et al. 2012). It should be noted that the initial concentrations of pollutants and the composition of the real water matrix also influence the efficiency of radiation-induced degradation. Consequently, gamma-induced removal of the target MPs varied significantly as a result of all these factors.

The efficiency of gamma radiation in the degradation of target MPs was also evaluated in terms of removal efficiency (%) as well as G-value, which is another index of the degradation of target compounds. Figure 8 illustrates the removal efficiency and G-value varying with different absorbed doses. From Fig. 8 and Table 5, it can be seen that IBF (0.304 μg $L^{-1}$) was efficiently degraded (86%) at a dose of 10 kGy. The removal efficiencies of DCF (0.227 μg $L^{-1}$), DPA (0.019 μg $L^{-1}$), TCS (0.567 μg $L^{-1}$), and BPA (0.578 μg $L^{-1}$) were 93, 79, 98, and 97%, respectively, at 20 kGy. On the other hand, KET (0.943 μg $L^{-1}$) and DEP (0.564 μg $L^{-1}$) were 78 and 83% degraded, respectively, after 30 kGy of exposure (Table 5, Fig. 8). It was found that although the removal efficiency increased as the absorbed dose increased, the G-value of the target MPs decreased. The decreased G-values indicated that there are lesser molecules being destroyed by applying increasing absorbed doses (Alsager et al. 2018). As can be seen from Fig. 8, the increase in removal efficiency was non-linear, indicating that removal of target MPs was rapid at low dose values, then slowed down at higher doses and reached a flat plateau at a certain dose value. This means that as the absorbed dose increased, the concentration of MP in the sample decreased, and the concentration reached a critical point where additional input energy could no longer destroy the target molecules. Consequentially, a decline in the G-value (decomposition yield) indicated a decrease in efficiency per unit of energy.

Since the radicals generated during water radiolysis are nonselective species, they undergo reactions with not only target molecules but also other components present in the sample. The decreasing trend of G-values with respect to absorbed dose might be due to the competitive reactions that occurred between the matrix components (dissolved organic substances, by-products, and inorganic ions) and the target MP molecules to react with the radicals produced by water radiolysis. In other words, with an increase in the absorbed dose and a decrease in the concentration of target MPs, the probability and rate of the reaction between reactive radicals and matrix components increase. In addition, the radical–radical recombination reactions, including radical ·OH, $e_{aq}^-$, and ·H (Eq. 10–13), could also contribute to the quenching of reactive species (Wang et al. 2019; Woods and Pikaev 1994).

$$\bullet OH + \bullet OH \rightarrow H_2O_2 \quad (10)$$

$$\bullet OH + \bullet H \rightarrow H_2O \quad (11)$$

$$\bullet OH + e_{aq}^- \rightarrow OH^- \quad (12)$$

$$\bullet H + e_{aq}^- \xrightarrow{H_2O} H_2 + OH^- \quad (13)$$

All of these factors resulted in a reduction of the effective concentration of radicals that react with the target MPs, thus lowering the G-value (Wang and Chu 2016; Boujelbane et al. 2022).

It was found that the relationship between $-\ln(C/C_0)$ and the absorbed dose is linear for all target MPs ($R$-squared values > 0.99), indicating that the degradation of MPs confirms to the pseudo first-order reaction kinetics (Boujelbane et al. 2022; Yao et al. 2023). Dose constants can be utilized to compare the removal efficiency between target MPs. For KET, DEP, DCF, and DPA, the dose constants ($k$, Eq. (7)), obtained by determining the slope of the lines of

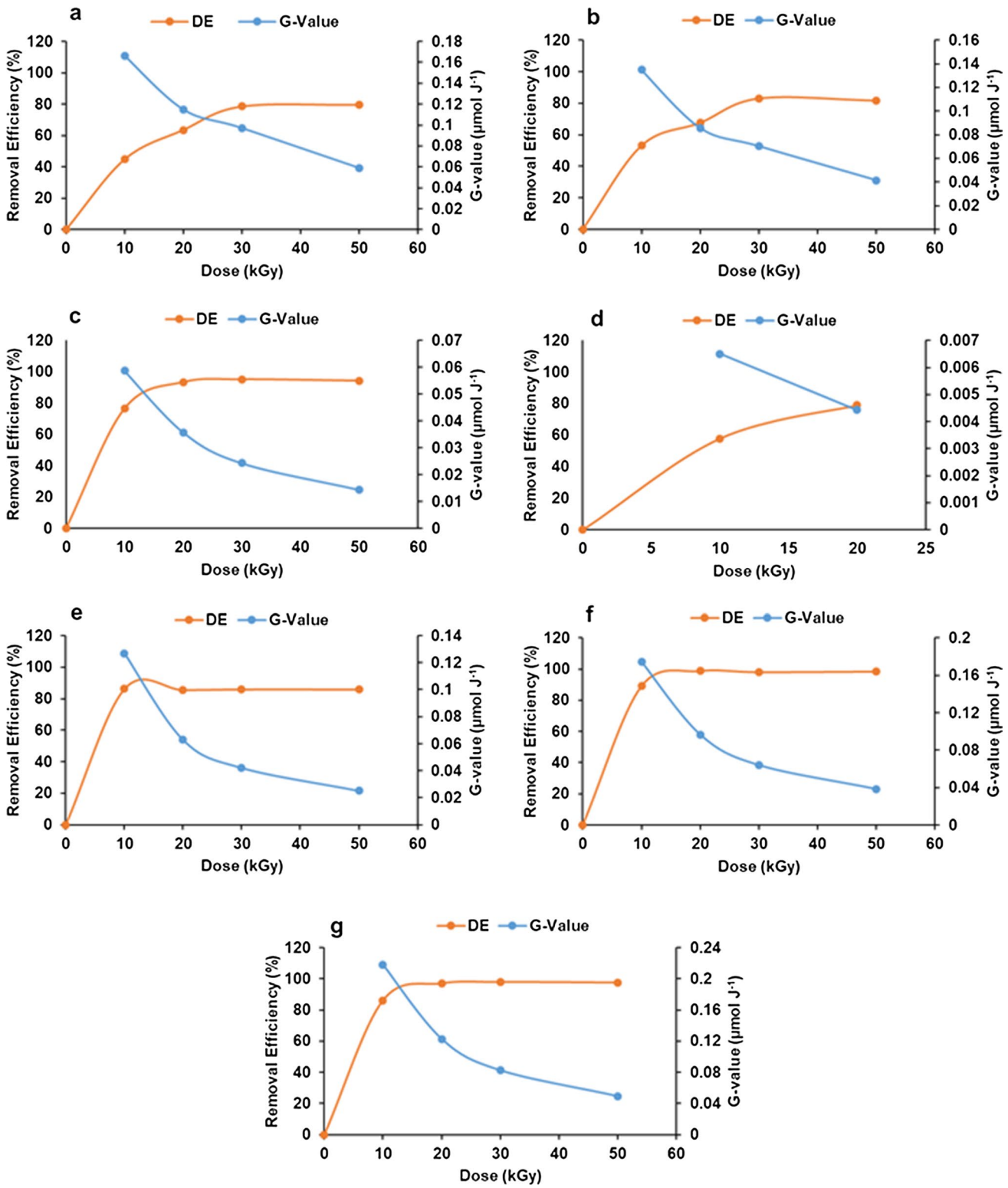


**Fig. 8** Percentage of removal and G-values of **a** KET, **b** DEP, **c** DCF, **d** DPA, **e** IBF, **f** TCS, and **g** BPA in function of the absorbed dose using gamma treatment

plots, correspond to 0.052, 0.057, 0.136, and 0.078 $kGy^{-1}$, respectively. For Group 2 compounds, *k* values were found to be 0.197 $kGy^{-1}$ for IBF, 0.219 $kGy^{-1}$ for TCS, and 0.176 $kGy^{-1}$ for BPA. These data indicate that TCS decomposes at a faster rate compared to other target MPs. This finding was supported by the calculations of $D_{0.5}$ and $D_{0.9}$ for the target MPs. For example, as shown in Table 5, 3.16 kGy was required for the 50% degradation of TCS, while the corresponding doses of $D_{0.5}$ for DCF and DEP were found to be 5.10 kGy and 12.14 kGy, respectively. Similarly, the lowest $D_{0.9}$ value among the MPs studied was found to be 10.49 kGy for TCS. Under the same irradiation conditions, the observed difference between the target MPs depends on their radiation stability, which is related to the structure of the molecules as well as their concentration. At this point, it should be noted that the $D_{0.9}$ values for KET, DEP, and IBF were calculated as 45.69, 40.32, and 11.67 kGy, respectively. However, at these dose values, the removal efficiencies of KET, DEP, and IBF were found to be approximately 79, 82, and 86%, respectively. The relatively low removal efficiencies obtained for KET, DEP, and IBF could probably arise from the competitive reactions mentioned previously. In addition, it should be taken into account that at high radiation doses, the probability of radical–radical recombination reactions increases, which reduces the concentrations of active radicals needed, particularly for the 90% degradation of KET and DEP.

Experiments performed using pure water spiked with MPs do not always give realistic results about the optimum irradiation dose for degradation due to the absence of matrix components and the spiking amounts that are incompatible with MP concentrations in real wastewater. For example, Kimura et al. (2012) dissolved some selected pharmaceuticals at 5 μmol $dm^{-3}$ concentration in real wastewater and found that DCF was decomposed at 1 kGy. However, in this study, the required doses for 90% removal of DCF ($7.67\times10^{-4}$ μmol $dm^{-3}$) could be achieved at approximately 17 kGy. Similarly, 10 mg $L^{-1}$ TCS prepared by adding directly to deionized water was removed 94% at an absorbed dose of 5 kGy (Wang and Wang 2017). On the other hand, the same percent removal efficiency was obtained at around 10 kGy in the present study. Table 6 summarizes the comparison of this study with the literature data available on the removal of some target MPs by gamma irradiation. These literature data are focused on the removal efficiency in pure water or real wastewater spiked with high MP concentrations. The higher dose values obtained in this study are due to the fact that the radiolytic species are consumed in wastewater by reacting with each other and/or with another matrix component until they diffuse and collide with very low concentrations of target MPs. In addition, the dose rate

**Table 6** The comparison of this study with the literature data available on the removal of some target MPs by gamma irradiation

| MPs | Initial concentration (mg/L) | Matrix | Irradiation dose(kGy) | Removal efficiency (%) | Refs. |
|---|---|---|---|---|---|
| KET | 101.9 | Water | 2.0 | 100.0 | Illes et al. 2012 |
| | 12.7 | Spiked in real wastewater | 2.0 | 100.0 | Kimura et al. 2012 |
| | $0.943\times10^{-3}$ | Real wastewater effluent | 30.0 | 78.6 | This study |
| DEP | 12.0 | Drinking water | 0.8 | 94.5 | Yongfu et al. 2012 |
| | $0.564\times10^{-3}$ | Real wastewater effluent | 30.0 | 83.2 | This study |
| DCF | 31.8 | Water | 1.0 | 100.0 | Homlok et al. 2011 |
| | 20.5–50.1 | Water | 0.9–1.2 | 90.0 | Liu et al. 2011 |
| | 15.9 | Spiked in real wastewater | 1.0 | 100 | Kimura et al. 2012 |
| | 50.0 | Deionized water | 3.6 | 95.0 | Bojanowska-Czajka et al. 2015 |
| | 4.5 | Ultrapure water | 1.01 | 95.0 | Nisar et al. 2016 |
| | 30.0 | Deionized water | 1.0 | 86.2 | Zhuan and Wang 2020 |
| | $0.227\times10^{-3}$ | Real wastewater effluent | 20.0 | 93.4 | This study |
| IBF | 28.3 | Ultrapure water | 1.1 | 100.0 | Zheng et al. 2011 |
| | $0.304\times10^{-3}$ | Real wastewater effluent | 10.0 | 86.2 | This study |
| TCS | 10.0 | Deionized water | 5.0 | 94.0 | Wang and Wang 2017 |
| | 8.0 | Distilled water | 0.6 | 100.0 | Zhang et al. 2021a |
| | $0.567\times10^{-3}$ | Real wastewater effluent | 20.0 | 98.8 | This study |
| BPA | 10.0 | Twice-distilled water | 8.0 | 98.0 | Guo et al. 2012 |
| | 20.0 | Ultrapure water | 0.7 | 98.1 | Rivera-Utrilla et al. 2016 |
| | 10.0 | Ultrapure water | 0.35 | 90.0 | Trojanowicz et al. 2021 |
| | $0.578\times10^{-3}$ | Real wastewater effluent | 20.0 | 97.1 | This study |

of the irradiator is another important factor for effective degradation (Getoff 2002).

These findings suggest that real parameters such as real samples, concentration of target compounds in the real sample, dose rate of the irradiator, and influence of matrix components should be taken into account in studies aiming for real industrial implementation of radiation technology. Otherwise, the optimum dose obtained for wastewater treatment may lead to misleading conclusions regarding the effectiveness of the irradiation process.

## Conclusions

This study investigated the removal of selected MPs commonly detected in wastewater effluents by ionizing radiation. An analytical methodology based on vortex-assisted liquid–liquid extraction followed by liquid chromatography with mass spectrometry was developed for the simultaneous determination of 13 MPs belonging to different classes. The proposed validated procedure provided high extraction efficiency ($\geq 96\%$) within a short extraction time (10 min), good linearity ($r^2 \geq 0.9990$) high accuracy (recovery = 94–109%) and precision (RSD $\leq 9\%$), and low limits of detection and quantitation (sub-μg $L^{-1}$ level). The developed analytical methodology was used for the determination of target MPs in wastewater effluent before and after irradiation.

When the wastewater effluent samples were subjected to gamma irradiation, the concentration of MPs showed a significant reduction at a dose of 10 kGy. Among the MPs studied, the lowest absorbed dose required for 90% removal was found for TCS (10.49 kGy). The removal efficiency of all target MPs increased with an increase in the absorbed dose. However, it was found that a higher absorbed dose was needed to remove target compounds in real wastewater samples compared to the studies performed using spiked samples, indicating that the character of the wastewater (the amount of pollutants as well as the presence of matrix components) has a significant influence on the removal efficiency. At this point, the importance of conducting research using real water samples has emerged in order to reveal real-world scenarios for the radiation-induced treatment of wastewater. In addition, since the pollutant concentrations and matrix components in each water body are different, the optimum dose required for the effective removal of pollutants and other operational parameters of the radiation technology implementation need to be determined for the real water sample. As a result, ionizing irradiation is a promising technology for the degradation of persistent pollutants in wastewater effluent.

**Supplementary Information** The online version contains supplementary material available at https://doi.org/10.1007/s11696-023-03168-6.

**Acknowledgements** This study has received research support from International Atomic Energy Agency (IAEA) through Radiation-Based Technologies for Treatment of Emerging Organic Pollutants CRP 23791 and Turkish Energy, Nuclear and Mineral Research Agency (TENMAK) (Irradiation Applications and Researches [A4.H1.F12]). This research is a part of Ms. Ayşenur Genç's PhD thesis. Ms. Genç is supported under YÖK 100/2000 PhD scholarship program-02.01.02. Molecular Pharmacology and Drug Investigation. The authors are thankful to Prof. Dr. Elif İnce and Prof. Dr. Özcan Yalçınkaya for constant motivation and support.

**Data availability** All data included in this study are available upon reasonable request from the corresponding author.

## Declarations

**Conflict of interest** The authors report there are no competing interests to declare.

## References

Ahmed SF, Mofijur M, Nuzhat S, Chowdhury AT, Rafa N, Uddin MA, Inayat A, Mahlia TMI, Ong HC, Chia WY, Show PL (2021) Recent developments in physical, biological, chemical, and hybrid treatment techniques for removing emerging contaminants from wastewater. J Hazard Mater 416:125912. https://doi.org/10.1016/j.jhazmat.2021.125912

Alsager OA, Alnajrani MN, Alhazzaa O (2018) Decomposition of antibiotics by gamma irradiation: kinetics, antimicrobial activity, and real application in food matrices. Chem Eng J 338:548–556. https://doi.org/10.1016/j.cej.2018.01.065

Aydin S, Aydin ME, Ulvi A, Kilic H (2019) Antibiotics in hospital effluents: occurrence, contribution to urban wastewater, removal in a wastewater treatment plant, and environmental risk assessment. Environ Sci Pollut Res 26:544–558. https://doi.org/10.1007/s11356-018-3563-0

Besha AT, Gebreyohannes AY, Tufa RA, Bekele DN, Curcio E, Giorno L (2017) Removal of emerging micropollutants by activated sludge process and membrane bioreactors and the effects of micropollutants on membrane fouling: a review. J Environ Chem Eng 5:2395–2414. https://doi.org/10.1016/j.jece.2017.04.027

Bezsenyi A, Sági G, Makó M, Palkó G, Tóth T, Wojnárovits L, Takács E (2020) The effect of combined cometabolism and gamma irradiation treatment on the biodegradability of diclofenac and sulfamethoxazole. Radiat Phys Chem 170:108642. https://doi.org/10.1016/j.radphyschem.2019.108642

Bhatt P, Bhandari G, Bilal M (2022) Occurrence, toxicity impacts and mitigation of emerging micropollutants in the aquatic environments: recent tendencies and perspectives. J Environ Chem Eng 10:107598. https://doi.org/10.1016/j.jece.2022.107598

Bírošová L, Lépesová K, Grabic R, Mackuľak T (2020) Non-antimicrobial pharmaceuticals can affect the development of antibiotic resistance in hospital wastewater. Environ Sci Pollut Res 27:13501–13511. https://doi.org/10.1007/s11356-020-07950-x

Bojanowska-Czajka A (2021) Application of radiation technology in removing endocrine micropollutants from waters and wastewaters—a review. Appl Sci 11:12032. https://doi.org/10.3390/app112412032

Bojanowska-Czajka A, Kciuk G, Gumiela M, Borowiecka S, Nałęcz-Jawecki G, Koc A, Garcia-Reyes JF, Ozbay DS, Trojanowicz

M (2015) Analytical, toxicological and kinetic investigation of decomposition of the drug diclofenac in waters and wastes using gamma radiation. Environ Sci Pollut Res 22:20255–20270. https://doi.org/10.1007/s11356-015-5236-6

Boujelbane F, Nasr K, Sadaoui H, Bui HM, Gantri F, Mzoughi N (2022) Decomposition mechanism of hydroxychloroquine in aqueous solution by gamma irradiation. Chem Pap 76:1777–1787. https://doi.org/10.1007/s11696-021-01969-1

Bujak IT, Pocrnić M, Blažek K, Bojanić K, Trebše P, Lebedev AT, Galić N (2023) Radiation-induced degradation of doxazosin: role of reactive species, toxicity, mineralization and degradation pathways. J Water Process Eng 51:103401. https://doi.org/10.1016/j.jwpe.2022.103401

Caban M, Migowska N, Stepnowski P, Kwiatkowski M, Kumirska J (2012) Matrix effects and recovery calculations in analyses of pharmaceuticals based on the determination of β-blockers and β-agonists in environmental samples. J Chromatogr A 1258:117–127. https://doi.org/10.1016/j.chroma.2012.08.029

Capodaglio AG (2020) Critical perspective on advanced treatment processes for water and wastewater: AOPs, ARPs, and AORPs. Appl Sci 10(13):4549. https://doi.org/10.3390/app10134549

Cárdenas H, Cartes M, Mejía A (2015) Atmospheric densities and interfacial tensions for 1-alkanol (1-butanol to 1-octanol)+water and ether (MTBE, ETBE, DIPE, TAME and THP)+water demixed mixtures. Fluid Phase Equilib 396:88–97. https://doi.org/10.1016/j.fluid.2015.03.040

Chavoshani A, Hashemi M, Amin MM, Ameta S (2020) Micropollutants and challenges: emerging in the aquatic environments and treatment processes. Elsevier, UK. https://doi.org/10.1016/B978-0-12-818612-1.00001-5

Chen X, Wang J (2020) Degradation of norfloxacin in aqueous solution by ionizing irradiation: kinetics, pathway and biological toxicity. Chem Eng J 395:125095. https://doi.org/10.1016/j.cej.2020.125095

Chu L, Wang J (2016) Degradation of 3-chloro-4-hydroxybenzoic acid in biological treated effluent by gamma irradiation. Radiat Phys Chem 119:194–199. https://doi.org/10.1016/j.radphyschem.2015.10.016

Chu L, Zhuan R, Chen D, Wang J, Shen Y (2019) Degradation of macrolide antibiotic erythromycin and reduction of antimicrobial activity using persulfate activated by gamma radiation in different water matrices. Chem Eng J 361:156–166. https://doi.org/10.1016/j.cej.2018.12.072

de Santiago-Martín A, Meffe R, Teijón G, Hernández VM, López-Heras I, Alonso CA, Romasanta MA, de Bustamante I (2020) Pharmaceuticals and trace metals in the surface water used for crop irrigation: risk to health or natural attenuation? Sci Total Environ 705:135825. https://doi.org/10.1016/j.scitotenv.2019.135825

Dong CD, Chen CW, Chen CF (2015) Seasonal and spatial distribution of 4-nonylphenol and 4-tert-octylphenol in the sediment of Kaohsiung Harbor. Taiwan Chemosphere 134:588–597. https://doi.org/10.1016/j.chemosphere.2014.10.082

Drzyzga O (2003) Diphenylamine and derivatives in the environment: a review. Chemosphere 53:809–818. https://doi.org/10.1016/S0045-6535(03)00613-1

Dueñas-Moreno J, Mora A, Cervantes-Avilés P, Mahlknecht J (2022) Groundwater contamination pathways of phthalates and bisphenol A: origin, characteristics, transport, and fate—a review. Environ Int 170:107550. https://doi.org/10.1016/j.envint.2022.107550

Getoff N (2002) Factors influencing the efficiency of radiation-induced degradation of water pollutants. Radiat Phys Chem 65:437–446. https://doi.org/10.1016/S0969-806X(02)00342-0

Ghazouani S, Boujelbane F, Ennigrou DJ, Van der Bruggen B, Mzoughi N (2022) Removal of tramadol hydrochloride, an emerging pollutant, from aqueous solution using gamma irradiation combined by nanofiltration. Process Saf Environ Prot 159:442–451. https://doi.org/10.1016/j.psep.2022.01.005

Guo Z, Dong Q, Zhang C (2012) Gamma radiation for treatment of bisphenol A solution in the presence of different additives. Chem Eng J 183:10–14. https://doi.org/10.1016/j.cej.2011.12.006

Gwenzi W, Chaukura N, Muisa-Zikali N, Musiyiwa K, Teta C (2022) Occurrence and behaviour of emerging organic contaminants in aquatic systems. In: Gwenzi W (ed) Emerging contaminants in the terrestrial-aquatic-atmosphere continuum. Elsevier, pp 67–86

Hina H, Nafees M, Ahmad T (2021) Treatment of industrial wastewater with gamma irradiation for removal of organic load in terms of biological and chemical oxygen demand. Heliyon 7(2):e05972. https://doi.org/10.1016/j.heliyon.2021.e05972

Homlok R, Takács E, Wojnárovits L (2011) Elimination of diclofenac from water using irradiation technology. Chemosphere 85(4):603–608. https://doi.org/10.1016/j.chemosphere.2011.06.101

Illés E, Takács E, Dombi A, Gajda-Schrantz K, Gonter K, Wojnárovits L (2012) Radiation induced degradation of ketoprofen in dilute aqueous solution. Radiat Phys Chem 81(9):1479–1483. https://doi.org/10.1016/j.radphyschem.2011.11.038

International Conference on Harmonization (ICH) of Technical Requirements for registration of Pharmaceuticals for Human Use (2005), Guideline Q2 (R1)-validation of analytical procedures: text and methodology, Geneva

Kecojević I, Đekić S, Lazović M, Mrkajić D, Baošić R, Lolić A (2021) Evaluation of LC-MS/MS methodology for determination of 179 multi-class pesticides in cabbage and rice by modified QuEChERS extraction. Food Control 123:107693. https://doi.org/10.1016/j.foodcont.2020.107693

Khan AH, Aziz HA, Khan NA, Hasan MA, Ahmed S, Farooqi IH, Dhingra A, Vambol V, Changani F, Yousefi M, Islam S, Mozaffari N, Mahtab MS (2022) Impact, disease outbreak and the eco-hazards associated with pharmaceutical residues: a critical review. Int J Environ Sci Technol 19:677–688. https://doi.org/10.1007/s13762-021-03158-9

Kim TH, Lee SH, Kim HY, Doudrick K, Yu S, Kim SD (2019) Decomposition of perfluorooctane sulfonate (PFOS) using a hybrid process with electron beam and chemical oxidants. Chem Eng J 316:1363–1370. https://doi.org/10.1016/j.cej.2018.10.195

Kimura A, Osawa M, Taguchi M (2012) Decomposition of persistent pharmaceuticals in wastewater by ionizing radiation. Radiat Phys Chem 81:1508–1512. https://doi.org/10.1016/j.radphyschem.2011.11.032

Kuckelkorn J, Redelstein R, Heide T, Kunze J, Maletz S, Waldmann P, Grummt T, Seiler TB, Hollert H (2018) A hierarchical testing strategy for micropollutants in drinking water regarding their potential endocrine-disrupting effects—towards health-related indicator values. Environ Sci Pollut Res 25:4051–4065. https://doi.org/10.1007/s11356-017-0155-3

Kumar R, Qureshi M, Vishwakarma DK, Al-Ansari N, Kuriqi A, Elbeltagi A, Saraswat A (2022) A review on emerging water contaminants and the application of sustainable removal technologies. Case Stud Chem Environ Eng 6:100219. https://doi.org/10.1016/j.cscee.2022.100219

Leito I, Herodes K, Huopolainen M, Virro K, Künnapas A, Kruve A, Tanne R (2008) Towards the electrospray ionization mass spectrometry ionization efficiency scale of organic compounds. Rapid Commun Mass Spectrom 22:379–384. https://doi.org/10.1002/rcm.3371

Liigand J, Laaniste A, Kruve A (2017) pH effects on electrospray ionization efficiency. J Am Soc Mass Spectrom 28:461–469. https://doi.org/10.1007/s13361-016-1563-1

Liu Q, Luo X, Zheng Z, Zheng B, Zhang J, Zhao Y, Yang X, Wang J, Wang L (2011) Factors that have an effect on degradation of diclofenac in aqueous solution by gamma ray irradiation.

Environ Sci Pollut Res 18:1243–1252. https://doi.org/10.1007/s11356-011-0457-9
Lord H, Pawliszyn J (2000) Microextraction of drugs. J Chromatogr A 902:17–63. https://doi.org/10.1016/S0021-9673(00)00836-0
Luo Y, Guo W, Ngo HH, Nghiem LD, Hai FI, Zhang J, Liang S, Wang XC (2014) A review on the occurrence of micropollutants in the aquatic environment and their fate and removal during wastewater treatment. Sci Total Environ 473–474:619–641. https://doi.org/10.1016/j.scitotenv.2013.12.065
Ma S, Jin X, Wei H, Liu Y, Guo M (2021) Hydrophobic deep eutectic solvent-based ultrasonic-assisted liquid–liquid micro-extraction combined with HPLC-FLD for diphenylamine determination in fruit. Food Addit Contam Part A 38:339–349. https://doi.org/10.1080/19440049.2020.1852320
Ma Y, Shen W, Tang T, Li Z, Dai R (2022) Environmental estrogens in surface water and their interaction with microalgae: a review. Sci Total Environ 807(1):150637. https://doi.org/10.1016/j.scitotenv.2021.150637
Morishima F, Inokuchi Y, Ebata T (2013) Structure and hydrogen-bonding ability of Estrogens studied in the gas phase. J Phys Chem A 117(50):13543–13555. https://doi.org/10.1021/jp407438j
Nisar J, Sayed M, Khan FU, Khan HM, Iqbal M, Khan RA, Anas M (2016) Gamma-irradiation induced degradation of diclofenac in aqueous solution: kinetics, role of reactive species and influence of natural water parameters. J Environ Chem Eng 4(2):2573–2584. https://doi.org/10.1016/j.jece.2016.04.034
Olaniyan LW, Mkwetshana N, Okoh AI (2016) Triclosan in water, implications for human and environmental health. Springerplus 5:1639. https://doi.org/10.1186/s40064-016-3287-x
Pisani E, Fattal E, Paris J, Ringard C, Rosilio V, Tsapis N (2008) Surfactant dependent morphology of polymeric capsules of perfluorooctyl bromide: influence of polymer adsorption at the dichloromethane–water interface. J Colloid Interface Sci 326(1):66–71. https://doi.org/10.1016/j.jcis.2008.07.013
Psillakis E (2019) Vortex-assisted liquid–liquid microextraction revisited. TrAC—Trends Anal Chem 113:332–339. https://doi.org/10.1016/j.trac.2018.11.007
Psillakis E, Kalogerakis N (2003) Developments in liquid-phase microextraction. TrAC—Trends Anal Chem 22:565–574. https://doi.org/10.1016/S0165-9936(03)01007-0
Rahimi-Nasrabadi M, Zahedi MM, Pourmortazavi SM, Heydari R, Rai H, Jazayeri J, Javidan A (2012) Simultaneous determination of carbazole-based explosives in environmental waters by dispersive liquid-liquid microextraction coupled to HPLC with UV-Vis detection. Microchim Acta 177:145–152. https://doi.org/10.1007/s00604-012-0762-0
Rivera-Utrilla J, Sánchez-Polo M, Ferro-García MÁ, Prados-Joya G, Ocampo-Pérez R (2013) Pharmaceuticals as emerging contaminants and their removal from water: a review. Chemosphere 93:1268–1287. https://doi.org/10.1016/j.chemosphere.2013.07.059
Rivera-Utrilla J, Sánchez-Polo M, Ocampo-Pérez R, López-Peñalver JJ, Velo-Gala I, Mota AJ (2016) Removal of compounds used as plasticizers and herbicides from water by means of gamma irradiation. Sci Total Environ 569:518–526. https://doi.org/10.1016/j.scitotenv.2016.06.114
Rizzo L, Malato S, Antakyali D, Beretsou VG, Đolić MB, Gernjak W, Heath E, Ivancev-Tumbas I, Karaolia P, Ribeiro ARL, Mascolo G, McArdell CS, Schaar H, Silva AMT, Fatta-Kassinos D (2019) Consolidated vs new advanced treatment methods for the removal of contaminants of emerging concern from urban wastewater. Sci Total Environ 655:986–1008. https://doi.org/10.1016/j.scitotenv.2018.11.265
Saadaoui H, Boujelbane F, Serairi R, Ncir S, Mzoughi N (2021) Transformation pathways and toxicity assessments of two triazole pesticides elimination by gamma irradiation in aqueous solution. Sep Purif Technol 276:119381. https://doi.org/10.1016/j.seppur.2021.119381
Senthilkumar A, Ganeshbabu M, Lazarus JK, Sevugarathinam S, John J, Ponnusamy SK, Chellam PV, Sillanpää M (2023) Thermal and radiation based catalytic activation of persulfate systems in the removal of micropollutants: a review. Ind Eng Chem Res 62(11):4554–4572. https://doi.org/10.1021/acs.iecr.2c02419
Shahid MZ, Usman MR, Akram MS, Khawaja SY, Afzal W (2017) Initial interfacial tension for various organic-water systems and study of the effect of solute concentration and temperature. J Chem Eng Data 62(4):1198–1203. https://doi.org/10.1021/acs.jced.6b00703
Shao Y, Chen Z, Hollert H, Zhou S, Deutschmann B, Seiler TB (2019) Toxicity of 10 organic micropollutants and their mixture: implications for aquatic risk assessment. Sci Total Environ 666:1273–1282. https://doi.org/10.1016/j.scitotenv.2019.02.047
Shin KA, Spain JC (2009) Pathway and evolutionary implications of diphenylamine biodegradation by *Burkholderia* sp. strain JS667. Appl Environ Microbiol 75:2694–2704. https://doi.org/10.1128/AEM.02198-08
Sievers M (2011) Advanced oxidation processes. In: Wilderer P (ed) Treatise on water science. Elsevier, pp 377–408
Stasinakis AS, Gatidou G (2010) Micropollutants and aquatic environment. In: Virkutyte J, Varma RS, Jegatheesan V (eds) Treatment of micropollutants in water and wastewater, 1st edn. IWA Publishing, London, pp 1–52
Tadros T, Izquierdo P, Esquena J, Solans C (2004) Formation and stability of nano-emulsions. Adv Colloid Interface Sci 108–109:303–318. https://doi.org/10.1016/j.cis.2003.10.023
Trojanowicz M (2020) Removal of persistent organic pollutants (POPs) from waters and wastewaters by the use of ionizing radiation. Sci Total Environ 718:134425. https://doi.org/10.1016/j.scitotenv.2019.134425
Trojanowicz M, Bojanowska-Czajka A, Szreder T, Męczyńska-Wielgosz S, Bobrowski K, Fornal E, Nichipor H (2021) Application of ionizing radiation for removal of endocrine disruptor bisphenol A from waters and wastewaters. Chem Eng J 403:126169. https://doi.org/10.1016/j.cej.2020.126169
Tyumina EA, Bazhutin GA, Cartagena Gómez ADP, Ivshina IB (2020) Nonsteroidal anti-inflammatory drugs as emerging contaminants. Microbiology 89:148–163. https://doi.org/10.1134/S0026261720020125
Välitalo P, Kruglova A, Mikola A, Vahala R (2017) Toxicological impacts of antibiotics on aquatic micro-organisms: a mini-review. Int J Hyg Environ 220(3):558–569. https://doi.org/10.1016/j.ijheh.2017.02.003
Varjani S, Sudha MC (2020) Occurrence and human health risk of micro-pollutants—A special focus on endocrine disruptor chemicals. In: Pandey A, Tyagi RD, Ngo HH, Larroche C (eds) Current developments in biotechnology and bioengineering. Elsevier, pp 23–39
Wang J, Chu L (2016) Irradiation treatment of pharmaceutical and personal care products (PPCPs) in water and wastewater: an overview. Radiat Phys Chem 125:56–64. https://doi.org/10.1016/j.radphyschem.2016.03.012
Wang S, Wang J (2017) Degradation of triclosan and its main intermediates during the combined irradiation and biological treatment. Environ Technol 39(9):1115–1122. https://doi.org/10.1080/09593330.2017.1321692
Wang J, Gong Z, Zhang T, Feng S, Wang JD, Zhang Y (2017) Simultaneous determination of 106 pesticides in nuts by LC–MS/MS using freeze-out combined with dispersive solid-phase extraction purification. J Sep Sci 40:2398–2405. https://doi.org/10.1002/jssc.201700092

Wang J, Zhuan R, Chu L (2019) The occurrence, distribution and degradation of antibiotics by ionizing radiation: an overview. Sci Total Environ 646:1385–1397. https://doi.org/10.1016/j.scitotenv.2018.07.415

Woods RJ, Pikaev AK (1994) Applied radiation chemistry: radiation processing. Wiley, New York

Yang XY, Qu Y, Yuan Q, Wan P, Du Z, Chen D, Wong C (2012) Effect of ammonium on liquid-and gas-phase protonation and deprotonation in electrospray ionization mass spectrometry. Analyst 138:659–665. https://doi.org/10.1039/C2AN36022E

Yao J, Rao W, Kong H, Sun W, Guo D, Li Z, Wei X (2023) Degradation of sulfamethoxazole in aqueous solution by low-energy X-ray irradiation. Catalysts 13:714. https://doi.org/10.3390/catal13040714

Yongfu Z, Zheng Z, Binguo Z, Changbao W, Lili L (2012) Removal of endocrine disruptors PAEs in drinking water by gamma-ray irradiation. Nucl Tech 35(9):680–685

Zhang Z, Chen H, Wang J, Zhang Y (2020) Degradation of carbamazepine by combined radiation and persulfate oxidation process. Radiat Phys Chem 170:108639. https://doi.org/10.1016/j.radphyschem.2019.108639

Zhang Z, Hu D, Chen H, Chen C, Zhang Y, He S, Wang J (2021a) Enhanced degradation of triclosan by gamma radiation with addition of persulfate. Radiat Phys Chem 180:109273. https://doi.org/10.1016/j.radphyschem.2020.109273

Zhang ZF, Zhang X, Zhang XM, Sverko E, Smyth SA, Li YF (2021b) Diphenylamine antioxidants in wastewater influent, effluent, biosolids and landfill leachate: contribution to environmental releases. Water Res 189:116602. https://doi.org/10.1016/j.watres.2020.116602

Zheng BG, Zheng Z, Zhang JB, Luo XZ, Wang JQ, Liu Q, Wang LH (2011) Degradation of the emerging contaminant ibuprofen in aqueous solution by gamma irradiation. Desalination 276(1–3):379–385. https://doi.org/10.1016/j.desal.2011.03.078

Zhuan R, Wang J (2020) Degradation of diclofenac in aqueous solution by ionizing radiation in the presence of humic acid. Sep Purif Technol 234:116079. https://doi.org/10.1016/j.seppur.2019.116079